Metrol. Meas. Syst., Vol. 32 (2025), No. 2
DOI: 10.24425/mms.2025.154341

POLSKA AKADEMIA NAUK

METROLOGY AND MEASUREMENT SYSTEMS

Index 330930, ISSN 0860-8229
www.metrology.wat.edu.pl

LEVERAGING THE TRANSPORTATION ALGORITHM FOR ENERGY FLOW OPTIMIZATION IN SMART HOUSEHOLDS

Piotr Powroźnik

University of Zielona Góra, Institute of Metrology, Electronics and Computer Science, prof. Z. Szafrana 2, 65-516 Zielona Góra, Poland
(✉ *p.powroznik@imei.uz.zgora.pl*)

Abstract

This paper presents the application of a transportation algorithm to optimize energy flow within a smart grid context. By leveraging this well-established optimization technique, it is demonstrated that energy efficiency and costs can be enhanced in individual households equipped with smart appliances and connected to both traditional and renewable energy sources. Simulation studies have shown that the algorithm can effectively determine optimal energy consumption patterns, leading to significant energy savings. Additionally, the algorithm can provide valuable insights into network congestion and energy demand forecasting, enabling distribution system operators to make informed decisions. The proposed solution aligns well with the concept of smart homes. By integrating with smart devices such as smart sockets and thermostats, energy consumption can be optimized based on real-time pricing and renewable energy availability, ultimately leading to lower energy bills and increased user comfort. Extending this approach to the distribution network level, by applying the transportation algorithm to optimize energy flow at the medium and low voltage levels, could further enhance grid stability and facilitate the integration of renewable energy sources.

Keywords: transportation theory, linear programming, elastic energy management, smart appliances, renewable energy sources, linear inequality constraints.

1. Introduction

The *phenomenon of peak demand* (PD) [1], characterized by a rapid increase in electricity demand within a short timeframe, poses a significant challenge to the stability of the *electric power system* (EPS). In a *smart grid* (SG) environment, this issue can be addressed through a variety of strategies aimed at optimizing energy consumption and enhancing network efficiency. One such approach is demand management, implemented through pricing programs that incentivize energy conservation and automation. Automation involves the deployment of intelligent systems to automatically curtail or limit the operation of electrical devices during peak load periods. Energy storage, the management of distributed energy generation, and the modernization of grid infrastructure also contribute to optimizing energy consumption and improving network efficiency.

The intermittent nature of *renewable energy sources* (RES) poses significant challenges for *distribution system operators* (DSOs). RES heavily rely on variable weather conditions and random natural phenomena. The unpredictability of weather patterns over extended periods makes it difficult to accurately forecast energy generation from these sources. Additionally, the geographic location of RES plays a crucial role. For instance, the efficiency of wind farms is highly dependent on local wind conditions, which can vary significantly even over short distances. Wind energy forecasting has been extensively studied [2]. *Photovoltaic* (PV) panels are susceptible to damage from overheating, necessitating the implementation of cooling systems [3]. During periods of high solar irradiance, PV systems can generate substantial

Article history: received August 26, 2024; revised November 9, 2024; accepted November 22, 2024; available online April 22, 2025.

amounts of electricity, potentially overwhelming the grid. Existing protection mechanisms often respond abruptly by disconnecting the PV system from the EPS. The criticality of this issue has been acknowledged through the development of simulation models [4] Additionally, the degradation of PV modules over time leads to a decline in efficiency, impacting overall energy generation capacity [5].

Energy harvesting has emerged as a promising approach in energy management [6]. Research has explored the extraction of energy from cantilever beams using piezoelectric materials [7]. Electronic circuits designed to power *Internet of Things* (IoT) sensors through the utilization of ambient energy have been developed [8]. Energy harvesting is increasingly recognized as a pivotal component of energy management strategies, particularly in the context of rising energy demand and the imperative to transition to sustainable energy sources.

Households equipped with *smart appliances* (SAs) offer opportunities for enhanced energy management. The benefits of SAs have been documented in previous research, including improvements in power quality and energy efficiency [9]. Algorithms for monitoring household energy consumption have been proposed, often employing *smart energy meters* (SEMs) to collect data at regular intervals [10]. Extensive research has been conducted on SEMs, encompassing a wide range of topics. Studies have focused on determining optimal inspection intervals for economic reasons [11] and leveraging SEM data for water consumption monitoring [12]. SEMs also play a crucial role in detecting energy theft [13], necessitating robust hardware and software security measures [14]. Recent advancements in SEM technology have enabled bidirectional communication, facilitating the exchange of electricity consumption data [15].

From the perspective of the SG, load levels, whether increased or decreased, should be distributed over extended periods. Energy deficiencies also pose a challenge. They often arise from heightened energy demand, particularly for heating, ventilation, and air conditioning (HVAC) systems [16]. This phenomenon is prevalent during summer and winter seasons, impacting user comfort as HVAC systems become indispensable. Beyond seasonal fluctuations, energy shortages may coincide with household activity patterns throughout the day, a characteristic often termed PD in the literature [1]. Household energy consumption typically peaks in the morning and afternoon due to daily routines such as cooking.

To maintain equilibrium between energy supply and demand, *distribution system operators* (DSOs) implement *elastic energy management algorithms* (EEM) [17] within the SG. Genetic algorithms offer a promising approach for EEM development [18]. The proposed solution is specifically designed for households, with all algorithmic operations executed within a SEM [19]. Leveraging the SEM's computational capabilities, additional functionalities for energy supply and demand management can be integrated. By estimating electricity consumption under nominal operating conditions of SA-equipped appliances and identifying extreme consumption values within specific timeframes, potential adjustments to electricity demand can be assessed. This information is crucial for DSOs in mitigating grid imbalances caused by energy surpluses, deficits, or discrepancies between supply and demand, particularly those arising from excessive RES generation. The article advocates for the application of *Transportation Theory* (TT) [20] to realize this solution.

This paper examines two-way communication between DSOs and households equipped with SEMs and SAs. A novel contribution is the quantification of potential electricity consumption adjustments within households. SEM-managed automation optimizes electricity costs by both reducing and increasing consumption, aligning with the growing demand for dynamic electricity tariffs. The ability to utilize household energy storage, such as electric vehicles, further enhances this solution.

DOI: 10.24425/mms.2025.154341

2. Methodology

Devices with SAs functionality offer the possibility of adjusting the power level at which they work (P_{SA}). The range of allowable modifications is specified by the manufacturer of a given SA. In this case, technical requirements are taken into account that will ensure the functionality of the given SA at the expense of reduced user comfort. This means, for example, reducing the power of, for example, a kettle, which will make it take longer to boil water. In a situation of excess energy, it is also possible to increase the power of the kettle. The set of all SAs available in the household is described by:

$$\Psi = \{\tilde{\Psi}_i\}_{i=1}^{N}, \tag{1}$$

where i is the index, N is the number of SAs.

On the other hand, the possible power selections for SA, which were specified by the manufacturer, are described using:

$$\bigwedge_{\substack{\tilde{\Psi}_i \in \Psi \\ i=1\ldots N}} \tilde{\Psi}_i = \{\psi_j\}_{j=1}^{L}, \tag{2}$$

where j is the index, L is the number of power settings for i-th SA.

To be more exact, the set of $\tilde{\Psi}_i$for selecting power settings for i-th SA can be written as follows:

$$\bigwedge_{\substack{\tilde{\Psi}_i \in \Psi \\ i=1\ldots N}} \tilde{\Psi}_i \in \{P_{\mathrm{SA}_{i_j}}\}_{j=1}^{L}. \tag{3}$$

In addition, for each $\tilde{\Psi}_i$ the dependency is provided by:

$$\bigwedge_{\substack{\tilde{\Psi}_i \in \Psi \\ i=1\ldots N}} \left(P_{\mathrm{SA}_{i_{\min}}} \in \tilde{\Psi}_i \wedge P_{\mathrm{SA}_{i_{\mathrm{nom}}}} \in \tilde{\Psi}_i \wedge P_{\mathrm{SA}_{i_{\max}}} \in \tilde{\Psi}_i\right) \tag{4}$$

Equation (4) specifies three power values for each i-th SA. These powers are related to the minimum ($P_{\mathrm{SA}_{i_{\min}}}$), nominal ($P_{\mathrm{SA}_{i_{\mathrm{nom}}}}$) and maximum ($P_{\mathrm{SA}_{i_{\max}}}$) operating mode with which a given SA works.

In the further part of the article, simulation studies will be devoted to the issue of obtaining estimation of the possibilities at a given moment of time (t). The research will concern the increase or decrease of the load level in a given SG. In particular, the considerations will concern households where user activities, e.g. cooking, are carried out on SAs devices. For the purpose of estimating the increase or decrease of the load level in the SG, a model was defined by describing the respective devices: R and S. R is understood as SAs, which are energy receivers (5). As an example R can be SA, for which it is possible to modify the power consumption. It can be a kettle, an electric stove or an air conditioner. Source of energy is understood as S (6). This group will include *conventional electricity suppliers* (CES), RES and energy storages (E). Taking into account the possibility of more than one E (7) in one household, a set was defined. The energy storage can be an energy storage for photovoltaics and also an electric car. Individual sets are described by (5), (6) and (7).

$$R = \{\mathrm{SA}_i\}_{i=1}^{N}, \tag{5}$$

$$S = \{\mathrm{CES,RES,E}\}, \tag{6}$$

$$E = \{\mathrm{ES}_j\}_{j=1}^{O}, \tag{7}$$

where O is the ES number.

The cardinality of the set R (5), S (6) and E (7) is: $N = |R|$, $M = |S|$ and $O = |E|$. For each element of the set E, the value of the maximum power P_{ES} [kW] (8) is assigned, which can be made available from individual ESs.

$$\bigwedge_{\substack{\mathrm{ES}_j \in \mathrm{E} \\ j=1\ldots O}} \mathrm{ES}_j = \left[P_{\mathrm{ES}_1}, \ldots, P_{\mathrm{ES}_O}\right] \tag{8}$$

In order to estimate the possibility of increasing or decreasing the load level in a given SG, TT was used.

3. The Transportation Theory implementation description

TT requires the determination of t at given time points: the shipment cost matrix $C(t)$ (9), the consumer demands vector $D(t)$ (10) and vector production capacities $H(t)$ (11).

$$C(t) = \begin{bmatrix} c_{1,1} & \cdots & c_{1,N} \\ \vdots & \ddots & \vdots \\ c_{M,1} & \cdots & c_{M,N} \end{bmatrix} \tag{9}$$

$$D(t) = [d_1, \ldots, d_N] = \left[\tilde{\psi}_1, \ldots, \tilde{\psi}_N\right] \tag{10}$$

$$H(t) = \begin{bmatrix} h_1 \\ \vdots \\ h_M \end{bmatrix} = \begin{bmatrix} P_{\mathrm{CES}} \\ P_{\mathrm{RES}} \\ H^{\top} \end{bmatrix} \tag{11}$$

The matrix $C(t)$ (9) contains the costs of supplying energy, depreciation between individual R and S. The consumer demands vector $D(t)$ contains the power level requirements, which must be offered by S for R. In this case, $D(t)$ will contain one power value from the set $\tilde{\Psi}_i$ (3) for i-th SA where $i = 1 \ldots N$. These values include $P_{\mathrm{SA}_{i_{\min}}}$, $P_{\mathrm{SA}_{i_{\mathrm{nom}}}}$, or $P_{\mathrm{SA}_{i_{\max}}}$ for i-th SA. Individual values of power settings from the $\tilde{\Psi}_i$ are based on the results from the assumptions of the manufacturer of a given SA so as to ensure the possibility of proper operation. The vector $H(t)$ (11) contains the determination of the power levels that can be delivered from each S. It was assumed that in the vector $H(t)$ (11) will be given the power values that can be offered by: CES (h_1), RES (h_2) and ESs ($[h_3, \ldots, h_M]^{\top}$). It was also assumed that there is only one CES per household. From the practical point of implementing a RES installation in a household, the value of P_{RES} will be the total value of power that was generated from all installations (e.g. PV or wind turbines). As ESs understood as classic stationary energy storage. The E set will also include the possibility of storing energy by electric cars. In order to protect the ESs against excessive discharge levels, the ξ minimum energy level coefficient below which the given ES cannot be unloaded. For this purpose, the vector Ξ (12) was defined.

$$\Xi = [\xi_1, \ldots, \xi_O] \tag{12}$$

In vector $H(t)$ (11) the correction of the unloading capacity of individual ESs is carried out using:

$$\bigwedge_{\substack{\alpha = P_{\mathrm{ES}_1}, \ldots, P_{\mathrm{ES}_O} \in H(t) \\ \beta \in \xi_{\mathrm{ES}_1}, \ldots, \xi_{\mathrm{ES}_O} \in \Xi \\ i=1\ldots O}} \alpha_i = \begin{cases} \alpha_i & \text{if } \alpha_i \geq \beta_i, \\ 0 & \text{otherwise.} \end{cases} \tag{13}$$

As a result of the operation of TT, solutions $X(t)$ (14) are obtained for subsequent time moments t.

$$X(t) = \begin{cases} \begin{bmatrix} x_{1,1} & \cdots & x_{1,N} \\ \vdots & \ddots & \vdots \\ x_{M,1} & \cdots & x_{M,N} \end{bmatrix} & \text{if } \sum_{i=1}^{M} h_i \geq \sum_{j=1}^{N} d_j, \\ \emptyset & \text{otherwise.} \end{cases} \tag{14}$$

In order to solve the problem of energy consumption estimation, the objective function of TT (15) was defined.

$$f_{\mathrm{TT}}(t) = \min_x \left\{ \bigwedge_{\substack{i,j\in\mathbb{N},\\ i=1\ldots M,\\ j=1\ldots N}} c_{i,j} x_{i,j} \right\} \tag{15}$$

Equation (15) is aimed at minimizing the costs of supplying power from a given S to each R. In practice, it will be possible to supply power first from RES, E, and in the absence of power, then and also from CES.

Solutions cannot be obtained by TT ($X(t) = \emptyset$) if power demand for R exceeds supply for S. If $X(t)) \neq \emptyset$, then the value of the solution x_{ij} is the power that will be delivered from S (h_i) to R (d_j). If $\sum_{i=1}^{M} h_i > \sum_{j=1}^{N} d_j$, it will mean that there will be unused production capacities ($\breve{H}(t)$) (16).

$$\breve{H}(t) = \begin{bmatrix} \breve{h}_1 \\ \vdots \\ \breve{h}_M \end{bmatrix} \tag{16}$$

The values of $\breve{h}_i$ mean unused power for *i*-th S. Similarly as for $H(t)$ (11), then in $\breve{H}(t)$ (16) the power values that have not been used are defined from: CES ($\breve{h}_1$), RES ($\breve{h}_2$) and ($[\breve{h}_3, \ldots, \breve{h}_M]^{\top}$). Individual $\breve{h}_i$ values are calculated using:

$$\bigwedge_{\substack{i\in\mathbb{N},\\ i=1\ldots M}} \breve{h}_i = h_i - \sum_{j=1}^{N} x_{i,j} \tag{17}$$

Excess RES power ($\breve{h}_2 > 0$) will be allocated to ESs boost in the first place. If all ESs are fully charged, the remaining power will be sold to CES. This problem can be solved with linear programming [21]. Linear inequality constraints [22] are written with:

$$\breve{x}_1 + \cdots + \breve{x}_O + \breve{x}_{O+1} \geq \breve{h}_2 \tag{18}$$

In linear inequality (18), $\breve{x}_{O+1}$ is the amount of excess power to be resold to CES. The remaining values of the $\breve{x}$ solutions refer to the power that is transferred to charge the individual ESs. In addition, boundaries are set with:

$$\begin{array}{ccccc} 0 & \leq & \breve{x}_1 & \leq & \dfrac{\sum_{j=1}^{N} c_{3,j}}{N} \\ & & \cdots & & \\ 0 & \leq & \breve{x}_O & \leq & \dfrac{\sum_{j=1}^{N} c_{k+2,j}}{N} \\ 0 & \leq & \breve{x}_{O+1} & \leq & \tau \end{array} \tag{19}$$

The value of τ from (19) is the maximum value of power that can be transferred to the SG. This value results directly from the contract signed with CES.

Solving the linear programming problem also requires specifying the objective function. In the case of power distribution for charging CES and ES, the objective function ($f_{\breve{h}_2}(t)$) is assigned the task of finding the minimum of the problem defined by:

$$f_{\breve{h}_2}(t) = \min_{\breve{x}} \left\{ \frac{\sum_{j=1}^{N} c_{3,j}}{N} \breve{x}_1 + \cdots + \frac{\sum_{j=1}^{N} c_{O+2,j}}{N} \breve{x}_k + \tau \breve{x}_{O+1} \right\} \tag{20}$$

The solutions of excess power distribution at a given moment t are written to the vector:

$$\breve{X}(t) = [\breve{x}_1 + \cdots + \breve{x}_O + \breve{x}_{O+1}] \tag{21}$$

Unused consumer demands $(\breve{D}(to))$ for the obtained solutions $X(t)$ (14) are described by:

$$\breve{D}(t) = \{\bigwedge_{\substack{j\in\mathbb{N},\\ j=1\ldots N}} \breve{d}_j : (d_j - \sum_{i=1}^{M} x_{i,j})\} \tag{22}$$

$X(t)$ (14) solutions are allowed by TT if $\sum_{i=1}^{M} \breve{d}_j = 0$. If $\sum_{i=1}^{M} \breve{d}_j \neq 0$ would mean that the required power was not provided for some SAs.

4. Simulation research

Thirteen SAs were used in simulation studies. Figure 1 shows a summary of P_{SA} profiles for thirteen SAs. Individual SAs may represent activities that are performed in a generic household. For example, it could be cooking or cleaning. P_{SA} draw values range up to 3.5 kW. The operation time of individual SAs is defined from several minutes to nearly two hours. Profiles of individual SAs were determined based on data collected in a household using the Voltcraft Energy Logger 4000 and Voltcraft SEM 8500 measurement devices. The collected data was imported into the MATLAB environment directly from the device or via the Tuya Smart platform for further analysis.

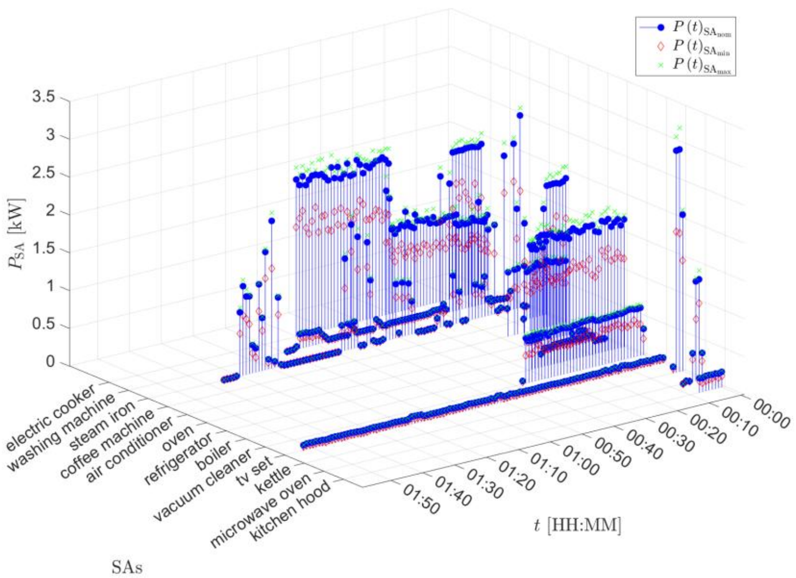

Fig. 1. Profiles for individual SAs.

Figure 2 shows the level of consumed energy $E(t)$ in individual hourly time intervals t. Based on the data presented in Fig. 2, it can be concluded that the operation of some of the SAs is characterized by periodic energy consumption. One such example of SAs is the boiler and refrigerator. A similar behavior in a narrower time interval is also characteristic of the air conditioner. For the remaining SAs, their mode of operation can be assigned to be triggered periodically. For the data presented in Fig. 1 the highest consumption of $E(t)$ in the morning and afternoon (T = {07:00, 08:00, 17:00, 18:00}). Individual hours from the T set result from everyday activities such as preparing meals or cleaning.

DOI: 10.24425/mms.2025.154341

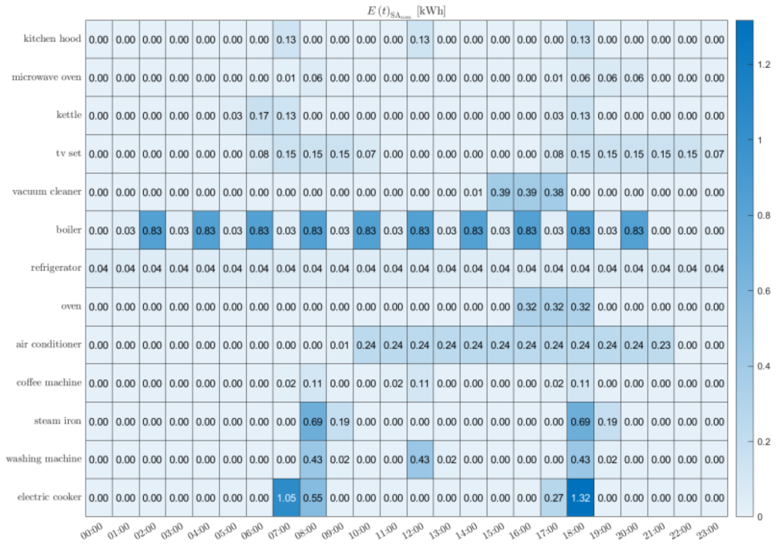

Fig. 2. Heatmap of the nominal energy consumption of individual SAs ($E(t)_{\mathrm{SA_{nom}}}$).

The summary of total power consumed in specific time intervals ($\sum P(t)_{\mathrm{SA}}$) is shown in Fig. 3. Individual values are grouped for three SAs operating modes: nominal ($P(t)_{\mathrm{SA_{nom}}}$), minimum ($P(t)_{\mathrm{SA_{min}}}$) and maximum ($P(t)_{\mathrm{SA_{max}}}$). The division into three modes provides the possibility of estimating the energy demand of the SAs during their operation in extreme and standard conditions. In order to conduct simulation research, uniformly distributed random numbers were used. Values ($P(t)_{\mathrm{SA_{min}}}$) and ($P(t)_{\mathrm{SA_{max}}}$) were determined using (24) and (25).

$$P(t)_{\mathrm{SA_{min}}} \sim U(0.9P(t)_{\mathrm{SA_{nom}}}, P(t)_{\mathrm{SA_{nom}}}) \tag{24}$$

$$P(t)_{\mathrm{SA_{max}}} \sim U(P(t)_{\mathrm{SA_{nom}}}, 1.15P(t)_{\mathrm{SA_{nom}}}) \tag{25}$$

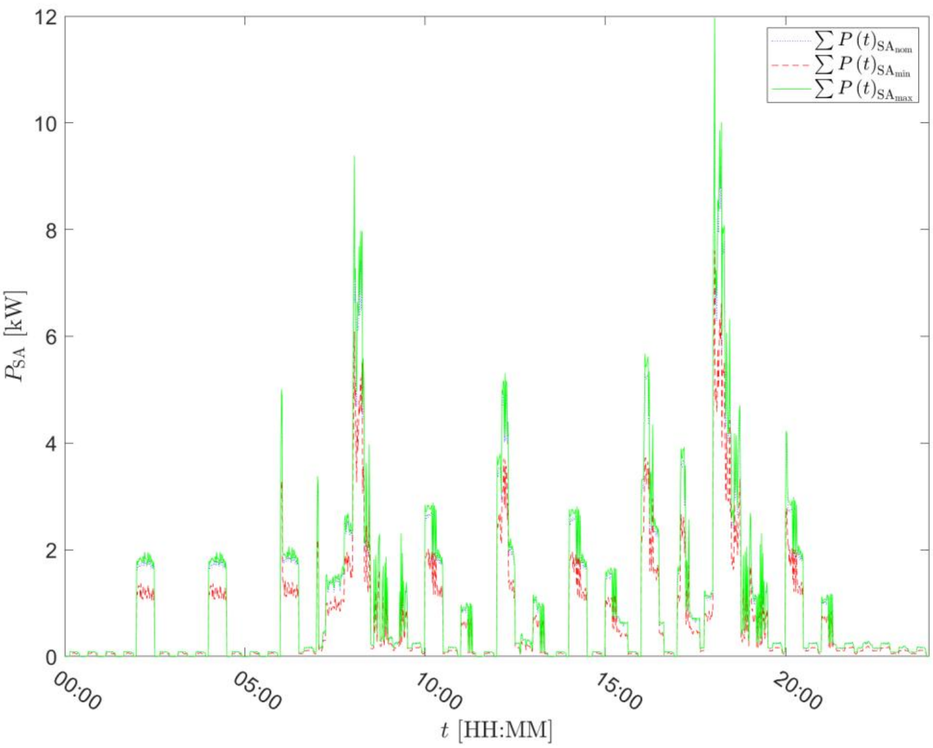

Fig. 3. List of $\sum P_{\mathrm{SA}}$ values at given times t, for three operating modes of SAs: nominal, minimum and maximum.

After determining $P(t)_{\mathrm{SA_{min}}}$ and $P(t)_{\mathrm{SA_{min}}}$ for individual SAs, the total power demand values were obtained for the minimum ($\sum P(t)_{\mathrm{SA_{min}}}$) and maximum ($\sum P)(t)_{\mathrm{SA_{max}}}$).

For the purpose of simulation research, the power from RES was additionally determined ($P(t)_{\mathrm{RES}}$). This value would be included in S. The $P(t)_{\mathrm{RES}}$ values shown in Fig. 4 were obtained for an example PV installation.

Simulation studies were carried out based on the TT algorithm. The implementation of the TT algorithm and simulation tests were carried out in the MATLAB environment. The idea of the TT algorithm is to ensure the possibility of correct operation R by the power available from all sources S.

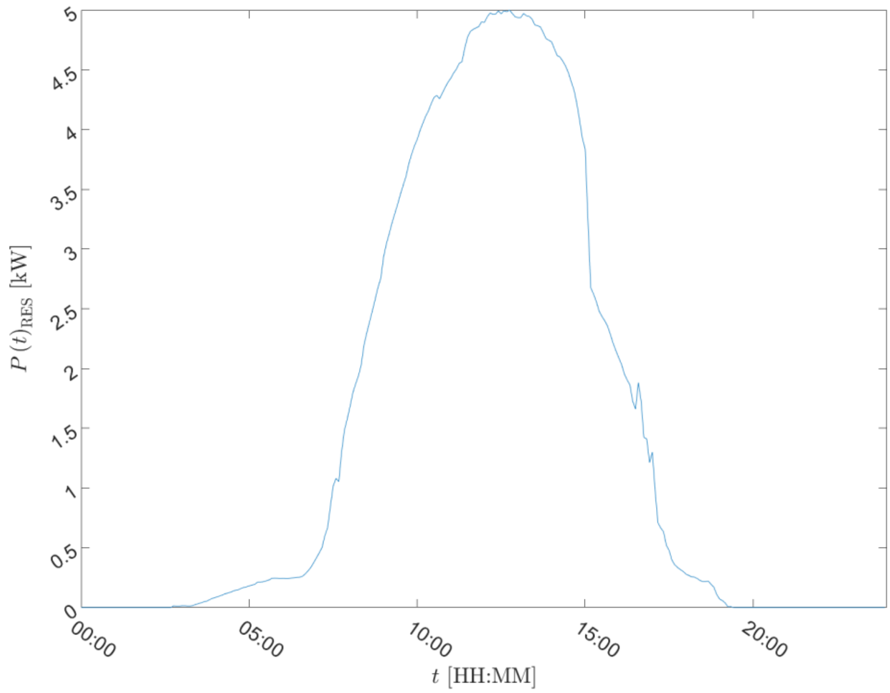

Fig. 4. Generation values $P(t)_{\mathrm{RES}}$ for the example PV.

For matrix $C(t)$ (9) the following assumptions were made:

$$\bigwedge_{\substack{c_{i,j}\in C(t)\\ j=1\ldots N}} c_{i,j} = \begin{cases} 0.99, & \text{if } i = 1,\\ 0.01, & \text{if } i = 2,\\ 0.05, & \text{if } i = 3,\\ 0.1, & \text{otherwise.} \end{cases} \tag{26}$$

The assumptions made for the cost function $C(t)$ (9) aimed to account for practical operational aspects. Specifically, we sought to model a scenario where the user prioritizes self-consumption of E, with selling to the DSO as a secondary option. Additionally, the goal was to determine the optimal sequence for utilizing different energy storage units in the system. The costs associated with E, incorporated into the $C(t)$ (9), primarily include life-cycle costs, related to battery degradation and the need for periodic replacement. Based on the adopted assumptions (26), it was ensured that the power from the RES would be taken first. Then, in case of power shortage from RES, the power will be taken from the available E. As for E, the sequence of charging and discharging of individual ESs was established. In this case, ES_1 was used first before ES_2. The following assumptions were also made as to the minimum energy level coefficient ξ below which a given ES cannot be discharged. In this case, the vector $\Xi = [0.2, 0.2]$.

Metrol. Meas. Syst., Vol. 32 (2025), No. 2
DOI: 10.24425/mms.2025.154341

The values of the vector consumer demands $D(t)$ (10) and the vector production capacities $H(t)$ (11) were different depending on a given time point *t*. The time set for simulation studies was defined by:

$$T = \{t_1, \dots, t_{1440}\} \Leftrightarrow \{00{:}00, 00{:}01, \dots, 23{:}59\} \tag{27}$$

Values of the vector consumer demands $D(t)$ (10) varied with respect to *t* and depended on the data adopted for simulation tests (Figs. 1, 2 and 3).

For the vector production capacities $H(t)$ (11) refer to $h_1 = 12$. This assumption corresponded to the possibility of obtaining power from CES of no more than 12 kW. The h_2 values were variable and depended on the power generation at a given time *t* from RES (Fig. 4).

The h_3 and h_4 values depended on the charge level of ES_1 and ES_2. The individual values of h_3 and h_4 were determined using:

$$\bigwedge_{\substack{\xi_i \in \Xi \\ h_{i+2} \in H(t) \\ i=\{1\dots k\}}} c_{i,j} = \begin{cases} 2.5, & \text{if } E_i \geq \xi_i E(\mathrm{ES}_i)_{\max}, \\ 0.0, & \text{otherwise.} \end{cases} \tag{28}$$

Individual values of 2.5 kW for ESs resulted from the example ES parameters. For the purposes of simulation tests, two ESs were selected with the following capacities: $E(\mathrm{ES}_1)_{\max}$ =5 [kWh] and $E(\mathrm{ES}_2)_{\max}$ =10 [kWh].

Figure 5 shows a histogram of the number of iterations of the TT algorithm needed to determine the way of power distribution from S to individual R. In most cases, the results were obtained for no more than five iterations.

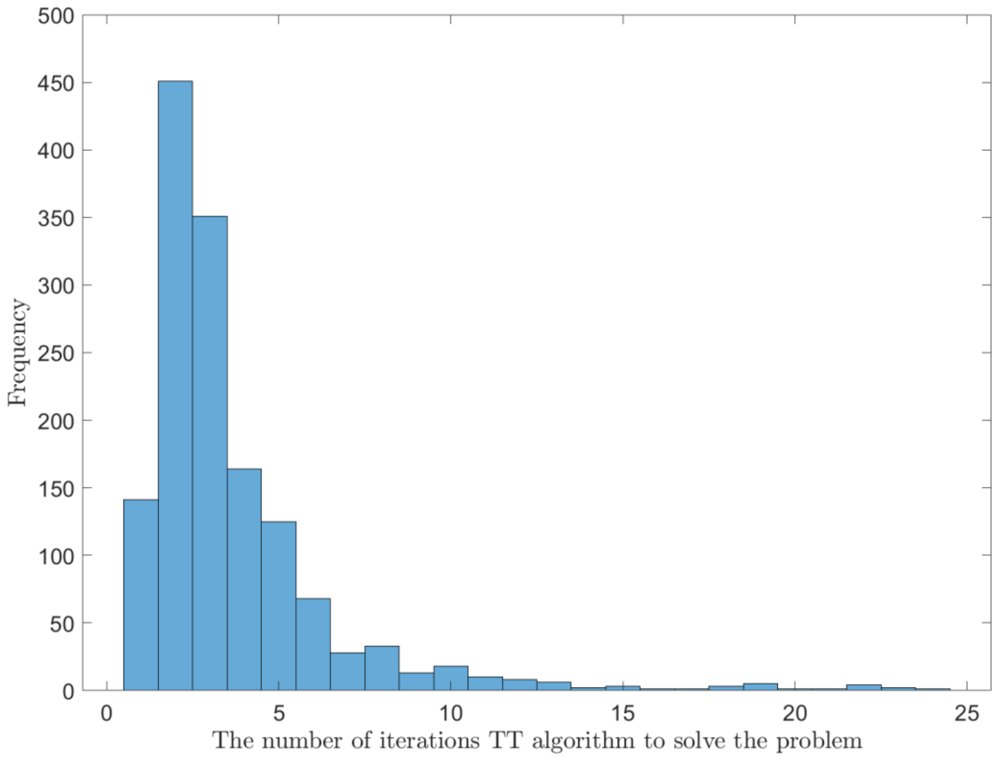

Fig. 5. Histogram of the number of iterations of the TT algorithm.

During the simulation tests, the charging and discharging characteristics of ES_1 and ES_2 were also determined. The characteristics are shown in Fig. 6. Within the respective time intervals, the effect of charging to the maximum capacity of a given ES and discharging it to the level of ξ can be observed. Determining which ESs are to be loaded is done using defined inequalities (19). In the case of simulation studies, ES_1 was defined as $\breve{x}_1$, and ES_2 was defined as $\breve{x}_2$. In the case of $\breve{x}_3 > 0$ (value $\breve{x}_{k+1}$ from (19) then there was excess power that had to be submitted to CES.

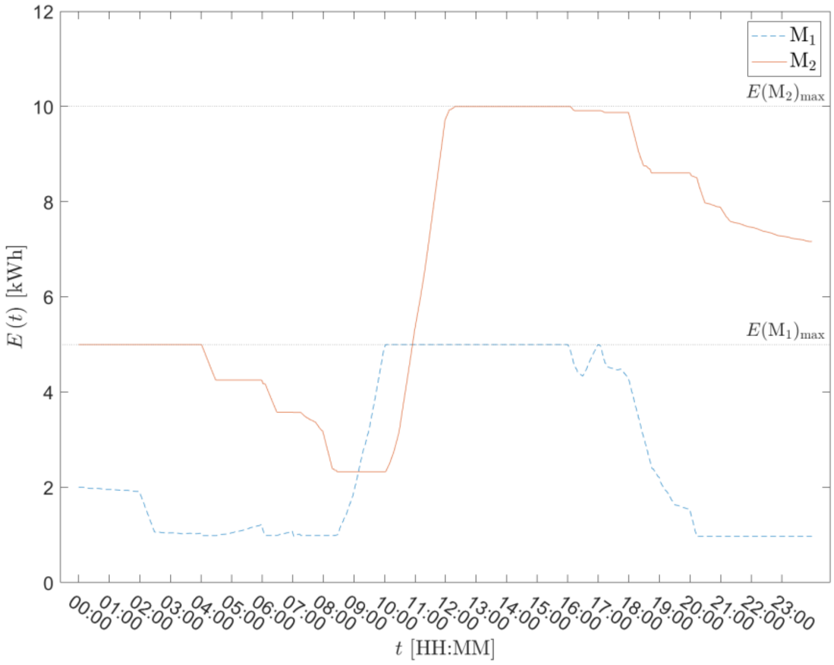

Fig. 6. Charging and discharging characteristics of ES_1 and ES_2.

In addition, Fig. 7 shows a situation where the excess energy produced from the RES could not be stored in two ESs. The energy had to be transferred (sold) to CES. This happened as $t = \{12:19, \dots, 16:00\}$.

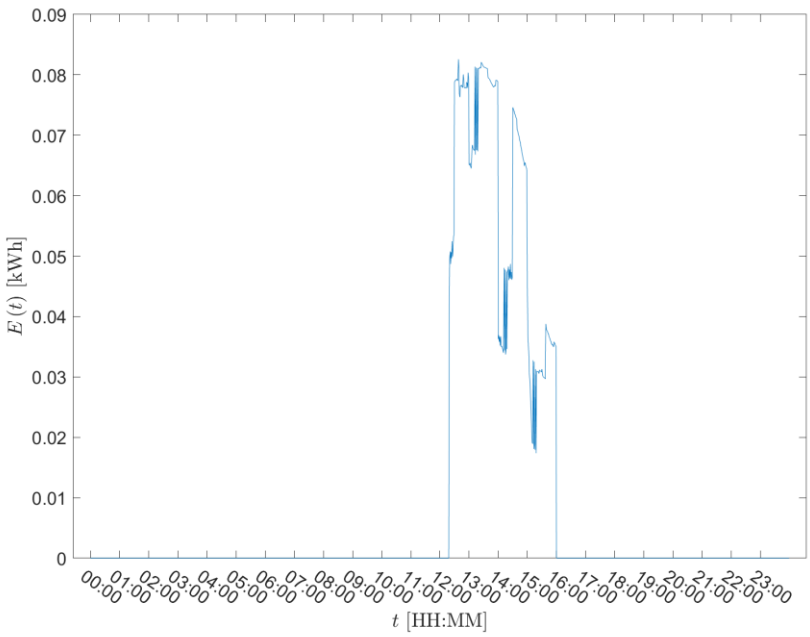

Fig. 7. Characteristics of selling excess energy $E(t)$ from RES that cannot be stored in ES_1 and ES_2.

Figure 8 shows detailed results of $X(t)$ (14) from the operation of the TT algorithm for $t =$ 18:08. The time moment t was selected for detailed analysis, among others, due to the increased demand for power by several SAs. In this case, it was necessary to provide power for all active

Metrol. Meas. Syst., Vol. 32 (2025), No. 2
DOI: 10.24425/mms.2025.154341

SAs from all S. The TT algorithm minimized the power consumption for $h_1 \in H(t)$ (CES) relative to the other S. For SA_6, SA_9 and SA_{12} found it necessary to supply power from two and three Ss respectively.

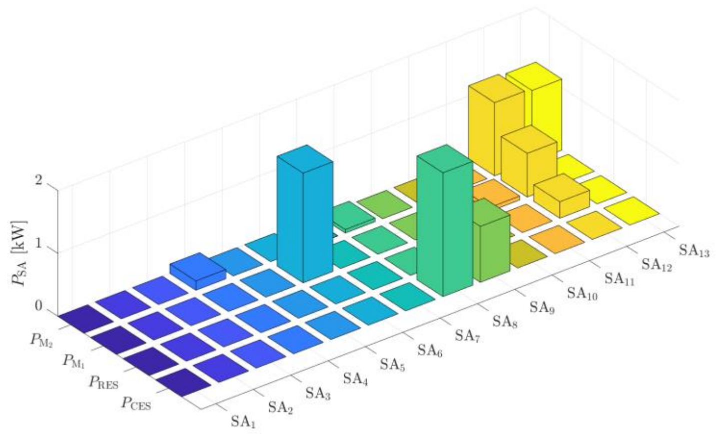

Fig. 8. Distribution of power from individual S to R at a given time $t = 18{:}08$.

In the next Fig. 9 again for $t = 18{:}08$ the results of the TT algorithm are presented. Figure 9 shows also the relationship between $X(t)$ and $\breve{D}(t)$. Based on the data presented in Fig. 9, it can be concluded that the TT algorithm correctly selected the values of $X(t)$, because all elements of the vector $\breve{D}(t)$ were equal to zero. It follows that consumer demands were fully met. For unused production capacities for $t = 18{:}08$, only $h_1 > 0$. In this case, the power consumption from P_{CES} was not fully utilised. Power from the remaining S was enough for R.

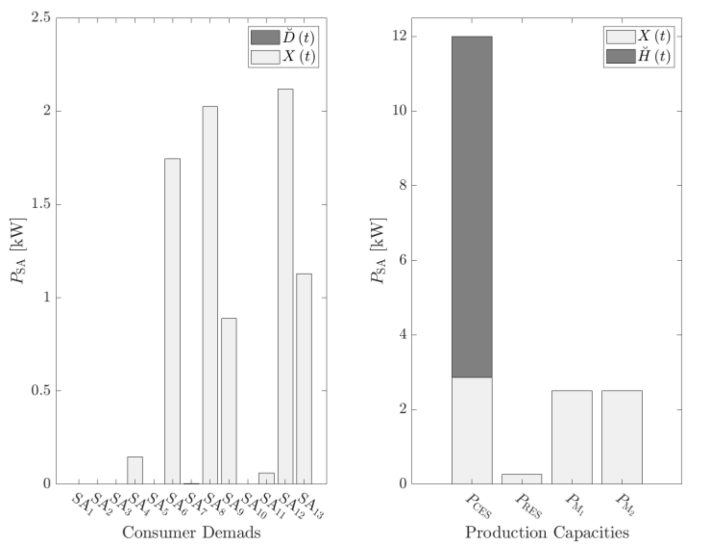

Fig. 9. Determination of consumption and reservation for *D* and *H*.

Figure 10 shows a summary of results for $X(t)$ and $X(t) + \breve{H}(t)$ obtained during the operation of TT algorithm. The obtained results were determined for the set T (27). Based on the data presented in Fig. 10, it can be confirmed that the TT algorithm first selected power consumption from RES, and only then from E. In the absence of power from RES and ES, only CES was selected.

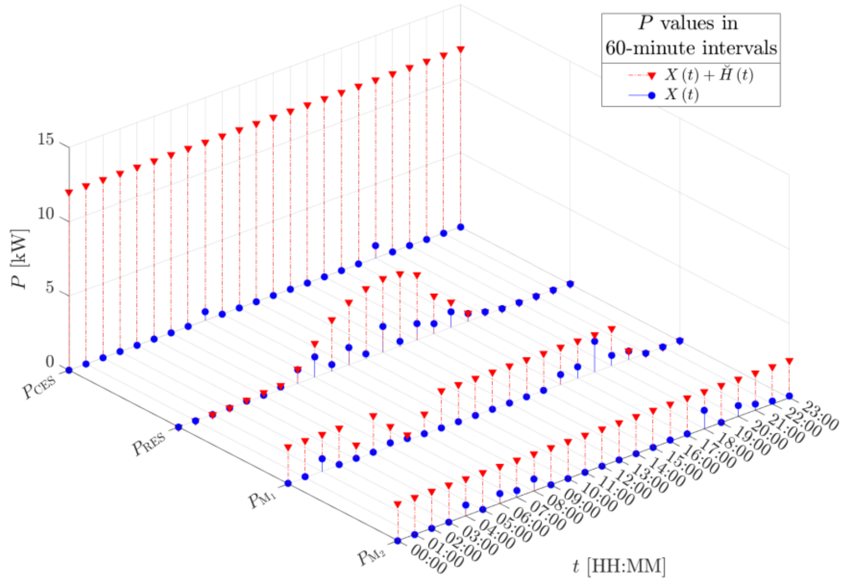

Fig. 10. Determination of consumption and reservation for *D* and *H*.

5. Conclusions

In the paper, an approach to estimate electricity consumption for EPS is presented. The estimation was made for households. Two groups were distinguished, S and R. For S, CES, RES and ESs were defined. In this case, ESs may be S as well as R. R is defined as the function of storing excess energy from RES so as not to transfer its excess to CES. As much energy will be transferred to CES as could not be stored in available ESs. This approach was aimed at reducing the risk of aperiodic EPS overload for many prosumers. As R, devices with SAs functionality were selected, for which it is possible to modify their operating mode. In the simulation studies carried out, three modes were focused: nominal, minimum and maximum. Selection of these modes enables energy consumption estimation for the full range of power consumption control possibilities. In this case, the elastic energy management algorithm, having data from individual layers of the SG, will be able to determine control decisions that will be transferred for execution. Selected values of energy consumption by sample SAs in the simulation studies were identified with activities that are performed during the day.

The conducted simulation studies took into account the specification of ESs, which can only be discharged to a certain level so that they are not damaged. For the purpose of conducting the research, an exemplary characteristic of energy generation from RES was analysed. Based on the results obtained from the simulation studies, the possibility of estimating the value of electricity consumption in a household using TT was confirmed.

The proposed TT algorithm is characterized by its simplicity and computational efficiency. A small number of computational steps required to achieve the optimal solution makes it an attractive alternative to more complex algorithms. The algorithm requires a small amount of input data, such as the shipment cost matrix matrix $C(t)$ (9), the consumer demand vector $D(t)$ (10), and the production capacity vector $H(t)$ (11). This allows it to be successfully implemented on devices with limited computational resources, such as smart electricity meters. The ability to communicate with other devices in a home network using the lightweight JSON format enables easy data exchange. Compared to other solutions, the proposed algorithm is characterized by a small number of iterations and a simple structure, which facilitates its implementation and analysis. The results provided by the algorithm can serve as a basis for further analysis, e.g., using machine learning algorithms. In a broader context, these algorithms can be used for energy production optimization, energy storage management, load balancing, demand management, distribution network optimization, integration of renewable energy sources, and data analysis and forecasting. The proposed solution fits perfectly into the concept of a smart home. An example of the benefits of its application is increasing user comfort through integration with systems that adjust lighting or temperature. Energy consumption optimization allows for reducing electricity bills by increasing energy consumption during periods when it is cheaper (e.g., as a result of excess energy from renewable sources) or reducing consumption by switching receivers to energy-saving mode. The proposed solution is a decision-making system based on measurement and control solutions, such as smart sockets or thermostats. Extending this solution to the distribution network level, by applying a transportation algorithm to optimize energy flow at the *medium voltage* (MV) and *low voltage* (LV) transformer level, would enable better management of renewable energy and increase network stability. The considerations presented in the article regarding the estimation of energy consumption in EPS networks can be extended to include an analysis of energy consumption by the industrial sector. This research topic is planned for future investigation. In particular, the considerations will concern households where user activities, such as cooking, are carried out on SAs. This research direction involves investigating human-computer interaction in cooking environments, designing intuitive interfaces for smart appliances, addressing privacy and security concerns, examining the impact of these devices on cooking habits and energy consumption, and exploring the specific characteristics of smart appliances.

6. References

[1] Masoud, F., Azah, M., Hussain, S., & Hadi, Z. (2013). Power quality impacts of high-penetration electric vehicle stations and renewable energy-based generators on power distribution systems. *Measurement*, *46*(8), 2423-2434. https://doi.org/10.1016/j.measurement.2013.04.032

[2] Prieto-Herráez, D., Martínez-Lastras, S., Frías-Paredes, L., Asensio, M. I., & González-Aguilera, D. (2024). EOLO, a wind energy forecaster based on public information and automatic learning for the Spanish Electricity Markets. *Measurement*, *231*, 114557. https://doi.org/10.1016/j.measurement.2024.114557

[3] Płachta, K., Mroczka, J., & Ostrowski, M. (2023). A new approach to water cooling of photovoltaic panels with a tracking system. *Metrology and Measurement Systems*, *30*(4), 675-687. https://doi.org/10.24425/mms.2023.147961

[4] Walczak, M., Bychto, L., Kraśniewski, J., & Duer, S. (2022). Design and evaluation of a low-cost solar simulator and measurement system for low-power photovoltaic panels. *Metrology and Measurement Systems*, *29*(4), 685-700. https://doi.org/10.24425/mms.2022.143067

[5] Mesbahi, O., Tlemçani, M., Janeiro, F. M., Hajjaji, A., & Kandoussi, K. (2021). Sensitivity analysis of a new approach to photovoltaic parameters extraction based on the total least squares method. *Metrology and Measurement Systems*, 28(4), 751-765. https://doi.org/10.24425/mms.2021.137707

[6] Moloudian, G., Hosseinifard, M., Kumar, S., Simorangkir, R. B., Buckley, J. L., Song, C., . . . O'Flynn, B. (2024). RF Energy Harvesting Techniques for Battery-Less Wireless Sensing, Industry 4.0, and Internet of Things: A Review. *IEEE Sensors Journal*, *24*(5), 5732-5745. https://doi.org/10.1109/JSEN.2024.3352402

[7] Dehghan Hamani, I., Tikani, R., Assadi, H., & Ziaei-Rad, S. (2020). Energy harvesting from moving harmonic and moving continuous mass traversing on a simply supported beam. *Measurement*, *150*, 107080. https://doi.org/10.1016/j.measurement.2019.107080

[8] Bouřa, A. (2020). A simple and affordable powering circuit for iot sensor nodes with energy harvesting. *Metrology and Measurement Systems, 27*(4), 575-587. https://doi.org/10.24425/mms.2020.134839

[9] Medina-Gracia, R., de Castro, A. d., Garrido-Zafra, J., Moreno-Munoz, A., & Cañete-Carmona, E. (2019). Power Quality Sensor for Smart Appliance's Self-Diagnosing Functionality. *IEEE Sensors Journal*, *19*(20), 9486-9495. https://doi.org/10.1109/JSEN.2019.2924574

[10] Ghosh, S., Manna, D., Chatterjee, A., & Chatterjee, D. (2021). Remote Appliance Load Monitoring and Identification in a Modern Residential System With Smart Meter Data. *IEEE Sensors Journal*, *21*(4), 5082-5090. https://doi.org/10.1109/JSEN.2020.3035057

[11] Radej, B., Drnovšek, J., & Begeš, G. (2019). Effect of environmental and operating conditions on the verification interval for smart electronic electricity meters. *Metrology and Measurement Systems*, *26*(1), 171-184. https://doi.org/10.24425/mms.2019.126328

[12] Koech, R., Gyasi-Agyei, Y., & Randall, T. (2018). The evolution of urban water metering and conservation in Australia. *Flow Measurement and Instrumentation*, *62*, 19-26. https://doi.org/10.1016/j.flowmeasinst.2018.03.011

[13] Qi, R., Zheng, J., Luo, Z., & Li, Q. (2022). A Novel Unsupervised Data-Driven Method for Electricity Theft Detection in AMI Using Observer Meters. *IEEE Transactions on Instrumentation and Measurement*, *71*, 1-10. https://doi.org/10.1109/TIM.2022.3189748

[14] Rincón, A. E., Melo, W. S., de Farias, C. M., & Carmo, L. F. (2021). Securing Smart Meters Through Physical Properties of Their Components. *IEEE Transactions on Instrumentation and Measurement*, *70*, 1-11. https://doi.org/10.1109/TIM.2020.3041098

[15] Klusacek, J., Langella, R., Meyer, J., & Drapela, J. (2024). Performance of Smart Revenue Meters Under Bidirectional Active Energy Flows in Energy Communities. *IEEE Transactions on Instrumentation and Measurement*, *73*, 1-12. https://doi.org/10.1109/TIM.2024.3382732

[16] Wang, Z., Yu, P., & Zhang, H. (2023). Privacy-Preserving Regulation Capacity Evaluation for HVAC Systems in Heterogeneous Buildings Based on Federated Learning and Transfer Learning. *IEEE Transactions on Smart Grid*, *14*(5), 3535-3549. https://doi.org/10.1109/TSG.2022.3231592

[17] Powroźnik, P., & Szcześniak, P. (2024). Energy Management of Home Devices With Smart Response for the Energy Generation Profile. *IEEE Transactions on Industrial Informatics*, *20*(4), 6995-7007. https://doi.org/10.1109/TII.2024.3353850

[18] Barszcz, T., & Zabaryłło, M. (2022). Automatic identification of malfunctions of large turbomachinery during transient states with genetic algorithm optimization. *Metrology and Measurement Systems*, *29*(1), 175-190. https://doi.org/10.24425/mms.2022.138551

[19] Flynn, C., Pengwah, A., Razzaghi, R., & Lachlan, A. L. (2023). An Improved Algorithm for Topology Identification of Distribution Networks Using Smart Meter Data and Its Application for Fault Detection. *IEEE Transactions on Smart Grid*, *14*(5), 3850-3861. https://doi.org/10.1109/TSG.2023.3239650

[20] Teodorovic, D., & Janic, M. (2022). Transportation Engineering: Theory, Practice, and Modeling. *Elsevier Science*. https://doi.org/10.1016/C2020-0-03714-X

[21] Ding, M., Yue, S., Song, K., & Wang, H. (2018). Fuzzy optimal solution of electric tomography imaging: Modelling and application. *Flow Measurement and Instrumentation*, *59*, 72-78. https://doi.org/10.1016/j.flowmeasinst.2017.11.012

[22] Li, H., Luo, Y., & Ai, D. (2023). Restoration of electromechanical admittance signature via solving constrained optimization problems for concrete structural damage identification. *Measurement*, *214*, 112803. https://doi.org/10.1016/j.measurement.2023.112803

Piotr Powroźnik received the M.Sc. degree in computer science from the University of Zielona Góra, Zielona Góra, Poland, in 2004, and the Ph.D. degree in electrical engineering from the Faculty of Electrical Engineering, Computer Science, and Telecommunications, University of Zielona Góra, in 2012. He is currently an Assistant Professor with the Institute of Metrology, Electronics, and Computer Science, University of Zielona Góra. His current research interests lie at the intersection of artificial intelligence and energy systems. He is particularly focused on leveraging advanced machine learning techniques, including deep learning, to address complex challenges in energy management and optimization. His research areas encompass: energy informatics, deep learning for energy systems, HVAC systems, hybrid electric vehicles, Industrial Internet of Things, NP-Hard problem solving and task scheduling in measurement and control systems.